TRANSACTIONS ON ELECTRICAL AND ELECTRONIC MATERIALS
Vol. 17, No. 6, pp. 341-350, December 25, 2016

Regular Paper

pISSN: 1229-7607 eISSN: 2092-7592
DOI: http://dx.doi.org/10.4313/TEEM.2016.17.6.341
OAK Central: http://central.oak.go.kr

# Power System Rotor Angle Stability Improvement via Coordinated Design of AVR, PSS2B, and TCSC-Based Damping Controller

Jamil Jannati†, Amin Yazdaninejadi, and Daryush Nazarpour
*Department of Electrical Engineering, Urmia University, Urmia, Iran*

**Received May 23, 2016; Revised August 18, 2016; Accepted August 19, 2016**

The current study is dedicated to design a novel coordinated controller to effectively increase power system rotor angle stability. In doing so, the coordinated design of an AVR (automatic voltage regulator), PSS2B, and TCSC (thyristor controlled series capacitor)-based POD (power oscillation damping) controller is proposed. Although the recently employed coordination between a CPSS (conventional power system stabilizer) and a TCSC-based POD controller has been shown to improve power system damping characteristics, neglecting the negative impact of existing high-gain AVR on the damping torque by considering its parameters as given values, may reduce the effectiveness of a CPSS-POD controller. Thus, using a technologically viable stabilizer such as PSS2B rather than the CPSS in a coordinated scheme with an AVR and POD controller can constitute a well-established design with a structure that as a high potential to significantly improve the rotor angle stability. The design procedure is formulated as an optimization problem in which the ITSE (integral of time multiplied squared error) performance index as an objective function is minimized by employing an IPSO (improved particle swarm optimization) algorithm to tune adjustable parameters. The robustness of the coordinated designs is guaranteed by concurrently considering some operating conditions in the optimization process. To evaluate the performance of the proposed controllers, eigenvalue analysis and time domain simulations were performed for different operating points and perturbations simulated on 2A4M (two-area four-machine) power systems in MATLAB/Simulink. The results reveal that surpassing improvement in damping of oscillations is achieved in comparison with the CPSS-TCSC coordination.

**Keywords:** Rotor angle stability, AVR, PSS2B, TCSC-based POD controller, IPSO algorithm

## 1. INTRODUCTION

Power system rotor angle stability is defined as the capability of a system to keep the transient stability in the first swing conception when subjected to a large-signal perturbation and also to keep the dynamic stability when it is retrieved from a small-signal perturbation [1,2]. In a multi-machine power system, the machine shaft angles, speeds, active and reactive powers, and terminal voltages are vulnerable signals at risk of multimodal EM (electromechanical) oscillations in the frequency range of 0.2 to 2 Hz due to insufficient damping torque in the system. More specifically, the inter-area oscillation occurs when large and distant power systems are joined together with weak tie-lines. This EM oscillation is revealed in the frequency range of 0.2 to 0.7 Hz, while the local oscillation occurs when the generators electrically near to each other oscillate locally in the frequency range of 0.7 to 2.0 Hz [3,4].

In order to improve the rotor angle stability different devices and complementary controllers can take part. In the current study, the engaged devices were 1) an AVR (automatic voltage regulator) of ST1A exciter, which is a common static excitation system, and 2) an advanced IEEE type dual-input power system stabilizer PSS2B, which is an add-on to the AVR in the presence

† Author to whom all correspondence should be addressed:
E-mail: J.Jannati@urmia.ac.ir

of a POD (power oscillation damping) controller based on a FACTS (flexible ac transmission system) such as TCSC (thyristor controlled series capacitor). A comprehensive review on the applications of PSSs in damping of power system oscillations utilizing PMUs (phasor measurement units) and wide-area measurements was undertaken in [5]. The transient stability can be affected easily by the AVR and TCSC, while the dynamic stability can be improved by the advanced PSSs with the lowest cost and best results. Uncoordinated and independent tuning of PSS and FACTS-based POD controller installed in an interconnected power system may lead to negative interactions between the controllers, in addition to limiting the operating range of the generators [6]. In earlier papers, the problem of coordination between conventional PSS (CPSS) - AVR controller [7-9] and between CPSS-FACTS based POD controller for improvement of multi-machine power system stability received much attention. In those papers, the main contribution was the advantage of coordinated design in comparison to individual design to improve damping performance of the power system, with the focus typically on applying dual-input stabilizers (P-w) PSS and PSS3B rather than CPSS in the coordination problem with UPFC and TCSC damping controllers to damp single machine infinite bus (SMIB) power system oscillations. An alternative was to focus on the coordinated design of AVR, (P-w) PSS, and TCSC-based POD controller to enhance SMIB system stability. However, in those studies, comprehensive coordination among AVR, PSS2B, and FACTS-based POD controller implemented on a practical multi-machine power system to enhance the rotor angle stability were not considered. In all of the published papers about CPSS-FACTS coordination, neglecting the proved adverse impact of a typical fast-response AVR on dynamic stability by disregarding AVR in the coordinated design process and so ignoring its gain reduction capability, had negative impacts on the effectiveness of the damping controllers. It has been proved in the literature that a fast-response AVR can produce positive synchronizing torque and negative electrical damping torque, which lead to improvement in the transient stability and destroy the oscillation stability [2,3,10]. Thus, in the proposed comprehensive coordination problem, taking the AVR as an adjustable controller instead of a fixed parameter device can attenuate the negative impacts indebted to its gain reduction capability and encourage the well-equipped system to work with high dynamical performance from the point of view of the rotor angle stability. Another advance of this comprehensive coordination study is the application of the advanced stabilizer in preference to CPSS. Although the machine active power or rotor speed signal can be considered separately as an input of a CPSS, it has been shown in the literature that in order to damp both local and inter-area oscillations effectively, two aforementioned signals should be employed together. The power signal characteristically deals with local disturbances and contains little information from the inter-area oscillation case, and is thus incapable of damping inter-area oscillations competently. Conversely the speed based stabilizer is inclined towards damping the inter-area oscillations. IEEE type dual-input PSS2B is constructed by synthesizing mentioned signals in such a way that it can be applied to damp the oscillations in a wide range of oscillation frequencies [11,12]. IEEE type PSS2B, called an integral of accelerating power stabilizer, comprises two chief components, namely a torsional filter and stabilizing parts. A further phase compensation block has been investigated in an updated version of the PSS2A model. This stabilizer can follow a low-speed ramp variation in mechanical power without any dc offset in output signal [12,13]. It has been concluded in [14] that a PSS2B stabilizer shows great damping performance in comparison with the CPSS.

In order to control power transfer in the transmission line rapidly via continuous controlling of the line reactance by series compensators, damping low frequency oscillations, and attenuating sub-synchronous resonance, the TCSC can be employed in tie-lines of poorly connected multi-area power systems as an economic series FACTS device with a complementary controller. Routine design and reliable control of a lead-lag structure and low cost are important reasons for why to date power industries feel satisfied with employing the linear lead-lag controllers to enhance the rotor angle stability [14,15].

Although the design of a stabilizer based on nonlinear control techniques, such as artificial intelligence, fuzzy logic, adaptive control, and neural networks, can yield robust design over wide changes in operating conditions, it is important to consider that the optimal adjustment of linear controllers under several operating conditions concurrently can provide remarkable robustness. Often, the coordinated design problem means concurrent tuning of the gains and time constants of the controllers considering the system operating constraints and desirable damping criteria to be fulfilled over presumed operating points.

In order to maximize the advantage of proposed controllers in the current paper, it was important to choose a powerful optimizing machine to tune the adjustable parameters properly. PSO (particle swarm optimization) algorithm is an evolutionary technique that is inspired from the social manner of bird crowds or fish herds in following swarm intelligence to find targets. PSO has been employed widely in optimization problems pertaining to PSS and FACTS POD controller coordinated design [15-17]. Furthermore, it can be coded in a few lines and executed quickly and precisely due to its effective optimizing process. In order to avoid untimely convergence PSO can achieve a balance between global and local explorations via controlling the self-learning and group-learning impacts of the speed updating rule of the particles [14]. An IPSO (improved PSO) algorithm has recently been introduced in [18] for a large diversity optimization problem, which employs crossover operators so that the search space can be easily and well surveyed. This helps in finding the global optimal solution more precisely.

In summary, the main novelties of this paper are as follows:

* For the first time, high-gain AVRs were incorporated in the coordinated design problem of PSSs and FACTS-based damping controllers to reduce the negative impact of the existing fixed parameters AVRs on the effectiveness of PSS-FACTS coordinated controller in improving the damping torque.
* A coordinated design was proposed of AVR, PSS2B, and TCSC-based POD (power oscillation damping) controller to effectively increase rotor angle stability of a multi-machine power system.
* A technologically viable stabilizer was employed, such as PSS2B rather than the CPSS in a coordinated scheme with AVR and POD controller to bring a well-established design with high potential structure to improve the rotor angle stability.
* A challenging performance index, called the ITSE (integral of time multiplied squared error), was considered to take maximum advantage of the considered controllers.
* An IPSO (improved PSO) algorithm reinforced by chaotic parameter and crossover operator was used to obtain a globally optimal solution.
* The robustness of the coordinated designs was guaranteed by regarding some operating conditions concurrently in the optimization process.

In the current paper a PSS2B dual-input stabilizer was used in a comprehensive coordination with an AVR and TCSC-based POD controller concurrently to provide high potential controller and

consequently to greatly improve the rotor angle stability of the commonly used 2A4M (2-area 4-machine) test system under both small and severe perturbations. The design problem was systematized as an optimization process in which the IPSO algorithm was applied to search the optimum gains and time constants by minimizing the ITSE (integral of time multiplied squared error) performance index as an objective function. In order to assure the robustness of the proposed coordinated controllers, the adjustable parameters were simultaneously tuned regarding some operating conditions. The effectiveness of the proposed controller AVR-PSS2B-POD was assessed via eigenvalue analysis and time domain simulations, compared to coordination of the CPSS-POD. Initial steps and the power system model under investigation is proposed in section two. Implementation of the proposed idea, participation factor analysis, parameters of coordinated control, formulating the problem, and numerical analysis is presented in section three and the last section concludes the paper.

## 2. POWER SYSTEM UNDER STUDY

In this part, the equipment of the 2A4M power system is described and dynamically modelled.

### 2.1 Power system stabilizers

In this section, the involved CPSS and PSS2B stabilizers are reviewed. All subsequent parameters are defined in the nomenclature at the end of the paper.

***A. CPSS (conventional power system stabilizer)***

In this work, the rotor speed signal is used as the CPSS input as seen in Fig. 1. The washout block TW is used to eliminate the dc output of the PSS when the system operates in the steady state condition. The lead-lag blocks are associated with T1 to T4 time constants provide the required phase lead [12].

Since the speed signal is easily affected by the noise, the speed

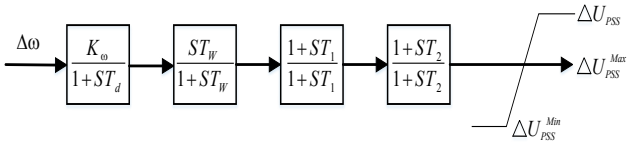


Fig. 1. CPSS (conventional power system stabilizer).

transducer should be precise and the time constant of the speed transducer Td should be sufficiently low in the case of oscillations damping by contributing to the CPSS [19].

***B. IEEE type PSS2B stabilizer***

Figure 2 shows the block diagram of the IEEE type PSS2B stabilizer. The fundamental layout was introduced in [3]. The PSS2B stabilizer consists of two main parts. In the first part, called filter part, the rotor speed and machine active power signals, which are obtained electrically, are combined to make a signal proportional

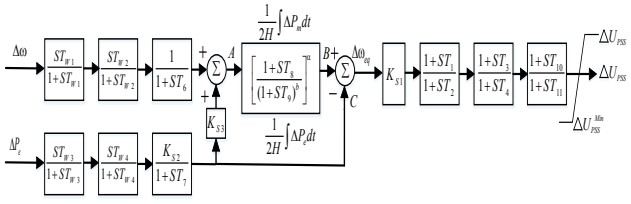


Fig. 2. IEEE type PSS2B stabilizer [12].

to the integral of the mechanical input power shown at A in Fig. 2. Subsequently, the provided signal is passed from the inner low-pass filter to attenuate the shaft torsional oscillation components. In the next step, the filtered signal located at point B is combined with the electrical counterpart signal available at point C to result in an equivalent speed signal at point D that is proportional to the integral of accelerating power as noticed in equation (1). Accordingly, the PSS2B stabilizer is commonly mentioned as the integral of accelerating power stabilizer in the literature. The second part of the PSS2B generates the stabilizing signal from the equivalent speed signal Δωeq without further washout block.

$$\Delta\omega_{eq} = \frac{1}{2H}\int(\Delta P_m - \Delta P_e)dt = \frac{1}{M}\int \Delta P_{acc}dt \tag{1}$$

The filter part parameters of the PSS2B can commonly be regarded as [4,12,20]: TW1 = TW2 =TW3 = T7 =10 sec; T6 ≈ 0; TW4 = 0; KS2 = T7 / (2H); KS3 = 1; a=1; b=5; T8=0.5 sec; T9= 0.1 sec. With these values, the stabilizer can tolerate a ramp change in the mechanical power without any dc output due to the internal ramp-tracking filter. This is useful since the mechanical power cannot be varied rapidly even for quick-acting valves. This property considerably decrease the terminal voltage modification under mandatory mechanical circumstances [12,21].

### 2.2 Two-area four-machine (2A4M) test system

The 2A4M system is shown in Fig. 3. It is embedded as the test system [3]. This test system is one of the common classic power systems in low frequency EM oscillations studies. The third-order model comprising the rotor swing equations (2), (3) and the internal voltage equation (4) are used to model synchronous machines, as outlined in [1]. Because of the simplicity of the classical model, it is satisfactory enough in studying low frequency oscillations. The two areas of the test 2A4M system (Area 1 and Area 2) are linked together by a 220 Km length tie-line, in which a power transfer exists from Area 1 to Area 2. Each area comprises two constant mechanical power synchronous generators with a rating of 900 MVA and 20 kV. In addition, they are equipped with IEEE type ST1A static excitation systems which include first order AVRs with transient gain reduction capability. The generators of the test system are connected to the 230 kV transmission lines with shown lengths by means of 900 MVA and 20/230 kV step-up transformers. Two constant impedance loads and two shunt capacitors are connected to the system at bus 11 and 12. The test system details and required data are given completely in [3].

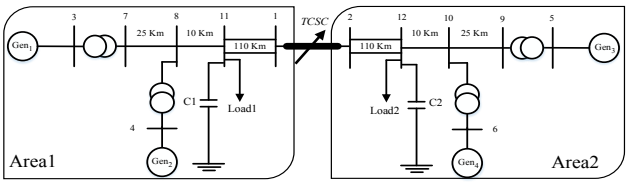


Fig. 3. 2A4M (two-area four-machine) system equipped with proposed controllers.

$$\frac{d\delta}{dt} = \omega_b(\omega - 1) \tag{2}$$

$$\frac{d\omega}{dt} = \frac{1}{M}(P_m - P_e - D(\omega - 1)) \tag{3}$$

$$\frac{dE'_q}{dt} = \frac{1}{T'_{do}}(E_{fd} - (x_d - x'_d)i_d - E'_q). \quad (4)$$

## 2.3 Excitation system model

In the network operating conditions, the static excitation system performs the very essential and important task of providing the stability of an interconnected power system because of its rapid acting capability to cause a high initial response to the variations. Often, a typical static excitation can provide more flexibility than brushless or dc excitation systems in reducing practical restrictions to expand the operating range of the power system and to exhibit more desired behaviour in the transient, steady state and dynamic conditions [12,22]. In this paper, to produce the dc field of the generators an IEEE type ST1A depicted in Fig. 4 was chosen because it is a fast-response excitation system with a very small inherent time constant. Moreover, it may be advantageous to decrease the high transient gain of the static excitation system for dynamical objectives [12,23].

The ST1A model is flexible to represent transient gain reduction fulfilled either by time constants TB and TC in a direct path (for this state, KF would set to zero) or by appropriate selection of KF and TF parameters in the feedback path [12]. The voltage regulator gain and inherent time constant of the excitation system are denoted by KA and TA, respectively. The time constants TC1 and TB1 represent the possibility of transient gain increase, which in our case meant that TC1 and TB1 should be set to zero. In many cases, the ceiling limitations on VI can be ignored [12]. Taking into account the above considerations and results from the literature [15], the simplified ST1A excitation system with transient gain reduction capability can be represented as Fig. 5 by taking into account TB1=TC1=0, KF=TF=0 [12].

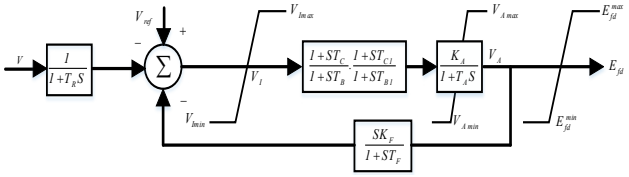

Fig. 4. IEEE type ST1A excitation system [12].

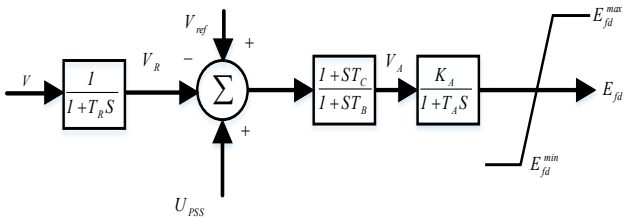

Fig. 5. Employed ST1A excitation system.

## 2.4 TCSC-based damping controller

The POD controller is designed to make available an electrical damping torque in phase with the speed deviation. As seen in Fig. 6, the conventional lead-lag structure is chosen for a TCSC-based POD controller. The determination of optimal location to install TCSC in the transmission line is commonly carried out by means of modal analysis techniques, such as the residue method [24]. Furthermore, the suitable choice of feedback signal for the FACTS-based POD controller was investigated in [25] to reach an effective and proper damping controller for inter-area oscillations. Since the main goal of the TCSC installation with POD controller in series with the transmission line is to control the active power flow and to damp inter-area low-frequency power swings effectively, the

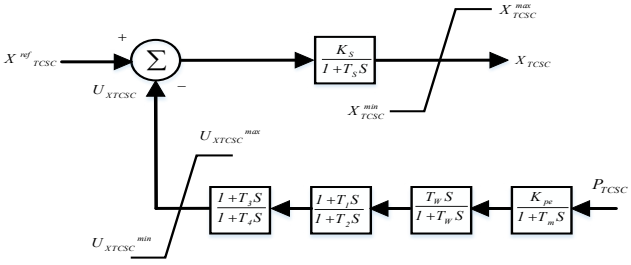

Fig. 6. TCSC-based POD controller.

TCSC is installed in the tie-line and the active power signal that contains useful information about the inter-area mode is considered as an effective local input of the POD controller [15].

In oscillation stability studies, the TCSC dynamic can be represented by:

$$\frac{dX_{TCSC}}{dt} = \frac{1}{T_S}(K_S(X^{ref}{}_{TCSC} - U_{XTCSC}) - X_{TCSC}) \quad (5)$$

The linearized model of the i[th] machine in a multi-machine power system equipped with the proposed ST1A excitation system, which is known as the modified Heffron-Phillips model, is shown in Fig. 7.

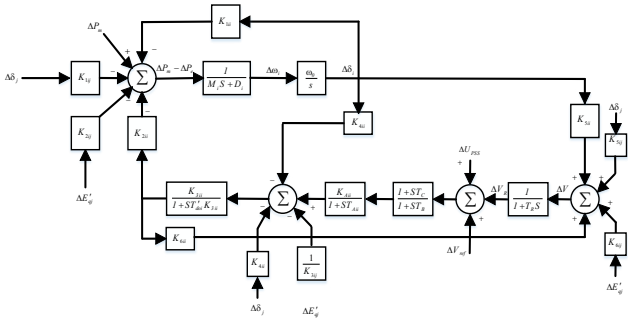

Fig. 7. Linearized model of the ith machine in multi-machine power system.

# 3. IMPLEMENTATION

In this part, the AVR-PSS2B-POD coordinated controller was designed using an improved PSO algorithm. Thereafter, its dynamic performance was compared with the CPSS-POD controller by eigenvalue analysis and various time domain simulations.

## 3.1 PF (participation factor) analysis

In order to design effective and proper damping controllers, it is important to identify modes of EM oscillation and catch the most affecting generators on the EM modes to determine the appropriate and suitable place for installing the stabilizers. Eigenvalue analysis of the base 2A4M system shows that, there are three EM modes; one in inter-area and two in local frequency ranges as shown in Table 1. It is obvious that the power system is unstable for inter-area mode due to positive real part or negative damping ratio.

In this study, the PF (participation factor) method was used to quantitatively evaluate the participation of state variables of the

Table 1. EM modes of the base 2A4M system.

| Operating condition | EM eigenvalue | Damping ratio ζ | Frequency (Hz) | EM type |
|---|---|---|---|---|
| Operating condition 1 [3] | 0.0232±3.0159i | -0.0077 | 0.4800 | Inter-area |
| | -0.7704±7.0459i | 0.1087 | 1.1214 | Local 1 |
| | -0.6789±6.8807i | 0.0982 | 1.0951 | Local 2 |

Table 2. Participation factor and mode shape analyses of the base 2A4M system.

| Local mode 2 | | Local mode 1 | | Inter-area mode | | State variables of generators |
|---|---|---|---|---|---|---|
| Participation factor | Mode shape | Participation factor | Mode shape | Participation factor | Mode shape | |
| 0.009 | 0.01 | 1.00 | 1.00 | 0.95 | 0.96 | $\Delta\delta_1$ |
| 0.012 | 0.02 | 0.98 | 0.99 | 0.92 | 0.93 | $\Delta\omega_1$ |
| 0.009 | 0.01 | 0.83 | 0.85 | 0.47 | 0.48 | $\Delta\delta_2$ |
| 0.015 | 0.02 | 0.80 | 0.82 | 0.44 | 0.45 | $\Delta\omega_2$ |
| 0.85 | 0.86 | 0.01 | 0.12 | 0.41 | 0.43 | $\Delta\delta_3$ |
| 0.82 | 0.83 | 0.02 | 0.11 | 0.43 | 0.44 | $\Delta\omega_3$ |
| 1.00 | 1.00 | 0.01 | 0.10 | 0.98 | 0.99 | $\Delta\delta_4$ |
| 0.98 | 0.99 | 0.01 | 0.009 | 0.96 | 0.97 | $\Delta\omega_4$ |

rotor angle and speed in the EM modes of the base 2A4M power system [3]. The optimal location to install the PSS is determined by evaluating the generators with the greatest PF and mode shape values related to the EM modes. It can be noticed from Table 2 that the generators 1 and 4 have the greatest values of PF and mode shape criteria. Thus, in order to enhance the damping of oscillations, the optimal places to install PSS are on generators 1 and 4.

## 3.2 Parameters of coordinated controllers

For the design problem of AVR-PSS2B-POD coordinated controller we concentrated on a simultaneous search for optimal adjustable parameters by IPSO algorithm by concurrently considering some operating conditions in the optimization process. The CPSS-POD coordinated controller was designed in a similar way to that reported in previous studies. The adjustable parameters of the coordinated controllers and the optimization range are shown in Table 3. In both coordinated controllers, all lead time constants (T1, T3, T10) should be adjusted above the given values of corresponding lag time constants (T2, T4, T11) to fully compensate for the phase lag in the excitation system [26]. The given parameters of the coordinated controllers are [12,26,27]: $T_m$=0.05 sec; $T_d$=0.02 sec; $T_W$=5 sec; $\Delta U_{PSS}^{max}$=-$\Delta U_{PSS}^{min}$=0.2 pu; $T_2$=$T_4$=$T_{11}$=$T_B$=0.1 sec; $T_{W1}$=$T_{W2}$=$T_{W3}$=10 sec; $T_{W4}$=0; $T_6$=0; $K_{S3}$=1; $K_{S2}$=$T_7$/(2H); a=1; b=5; $T_8$=0.5; $T_9$=0.1; $T_R$=0.02 sec. Besides, for CPSS-POD controller: $K_A$=210; $T_A$=0 sec; $T_B$=$T_C$=1 [3].

## 3.3 Proposed objective function for optimal PSS design

In order to obtain a robust coordinated controller, the adjustable parameters should be optimized over various operating conditions simultaneously. The ITSE performance index penalizes the error more than the ITAE; hence, this minimizes the chance of large peak error more than the ITAE index due to the higher power of error term. Also, due to the time factor, the settling time is shorter than with application of the ISE index [28]. In this study, the ITSE index is given as:

$$ITSE = \sum_{i=1}^{n}\int_0^{T_{sim}} t[\sum(\Delta\omega_L)^2 + \sum(\Delta\omega_I)^2]dt \quad (6)$$

Where Tsim denotes the simulation time; ΔωI and ΔωL stand for the speed deviations of inter-area and local modes, correspondingly; and n is sum of operating points considered in the robust design. The minimization of (6) leads to damping in all local and inter-area mode oscillations. The ITSE index uses properties of both ISE (integral of squared error) and ITAE (integral of time absolute error) indices as it uses squared error and time to weight vast oscillations and penalize long settling times.

The design problem is to minimize the ITSE index subject to constraints related to the adjustable parameters.

## 3.4 IPSO (improved particle swarm optimization) algorithm

PSO (particle swarm optimization) is a member of a wide category of swarm intelligence-based optimization algorithms. PSO as an optimization machine is one of the most well-known heuristic evolutionary algorithms, which have found many applications in solving engineering optimization problems. Recently, in the case of populations with large diversity, an IPSO (improved PSO) algorithm has been presented in [18], which also have crossover operators, hence enabling the search space to be well surveyed. This fact helps in discovering the global optimal solution with greater confidence. IPSO is used here to minimize the ITSE objective function for its convergence effectiveness in optimizing the parameters. To determine optimal parameters of the controllers, the IPSO should explore in multi-dimensional search space. To start the optimization process initially some executions

Table 3. Adjustable parameters of coordinated controllers and optimization range.

| Coordinated controllers | Adjustable parameters | Optimization range of adjustable parameters | | |
|---|---|---|---|---|
| AVR-PSS2B-POD | $K_A$, $K_{pe}$ , $K_{S1}$, $T_1$, $T_3$, $T_{10}$, $T_A$, $T_B$, $T_C$ | $0.1<T_1,T_3,T_{10}<1$ $0<T_B,T_C<1$ | $0.01<K_{pe},K_{S1}<100$ | $100<K_A<250$ $0.001<T_A<0.1$ |
| CPSS-POD | $K_{pe}$, $K_\omega$, $T_1$, $T_3$ | $0.1<T_1,T_3<1$ | $0.01<K_{pe},K_\omega<100$ | $K_A$=200, $T_A$=0.01 |

were performed with different values of the IPSO parameters to assess if the IPSO would find satisfactory results or not. The parameters of the IPSO algorithm should be selected carefully to ensure high performance. The parameters for MATLAB-based IPSO program are chosen as: n=30; m=6; $\omega_{min}$=0.4; $\omega_{max}$=0.9; c1=c2=2; λ=0.1; $t_{max}$ =30; $C_R$=0.6, where n is the population size; m is total number of parameters to be optimized; $\omega_{max}$, $\omega_{min}$ are the initial and final inertia weights; c1, c2 are acceleration coefficients; λ is a chosen number in interval (0, 1) to control the maximum vector of velocity; $t_{max}$ is total number of the iterations; and CR is crossover rate. For more information about PSO and IPSO algorithms it is better to refer to [14,29,30].

## 3.5 Eigenvalue analysis

Eigenvalue analysis can be a quantitative method to evaluate the dynamic stability of the power system in determining the damping ratio and damping coefficient or other stability measurement indices. In order to achieve robust controllers three operating points, given in Table 4, were considered in the robust design process. To start the optimization process initially some executions were performed with different values of the IPSO parameters to assess the performance to determine whether the parameters would produce satisfactory results or not. The parameters of the algorithm should be selected carefully to provide a high-performance IPSO algorithm.

Table 5 lists final adjusted parameters of the various coordinated controllers obtained by the PSO algorithm. It can be seen in Table 5 that the optimized gain and time constant of AVR in our proposed coordinated controllers are smaller than where the AVR parameters are considered fixed ($K_A$=200 , $T_A$=0.01). In fact, we use the transient gain reduction capability of the ST1A excitation system by involving AVR in the coordinated design. The decreased gain can be very effective in reducing the negative impact of AVR on the dynamic stability. Furthermore, the smaller time constant can bring about a faster response of AVR in transient conditions. These significant results can help in improving the power system rotor angle stability.Figure 8 shows the convergence rate of the objective function where the proposed coordinated controller has been optimized. It can be easily seen that the AVR-PSS2B-POD coordinated controller has been adjusted with a smaller cost value compared with other designs. This matter may be interpreted as the higher damping performance of the proposed coordination. Since it is obvious from the objective function that the damping ratios and damping coefficients are improved as much as possible, a small cost of the design can be obtained. This may result in great performance and capability of the proposed controller to reach the design aims.

Table 6 lists the EM modes of the 2A4M system for two different operating conditions 1 and 3 with and without the proposed coordinated controllers. The damping ratio appears to be an appropriate quantitative measurement to estimate the damping characteristics of the EM oscillation mode. As it can be seen in Table 1, the base 2A4M power system reveals two poorly damped local modes and one unstable inter-area mode.

Table 5. Adjusted parameters obtained by the PSO algorithm.

| | CPSS-POD | | AVR-PSS2B-POD | | |
|---|---|---|---|---|---|
| | CPSS | POD | AVR | PSS2B | POD |
| $K_A$ | - | - | 185.88 | - | - |
| $K_{Pe}$ | - | 0.2102 | - | - | 0.0445 |
| $K_\omega$ | 0.1231 | - | - | - | - |
| $K_{S1}$ | - | - | - | 0.0529 | - |
| $T_1$ | 0.3477 | 0.1123 | - | 0.1928 | 0.3228 |
| $T_3$ | 0.2437 | 0.3416 | - | 0.2250 | 0.5493 |
| $T_{10}$ | - | - | - | 0.3796 | - |
| $T_A$ | - | - | 0.0080 | - | - |
| $T_C$ | - | - | 0.3500 | - | - |
| $T_B$ | - | - | 0.1321 | - | - |

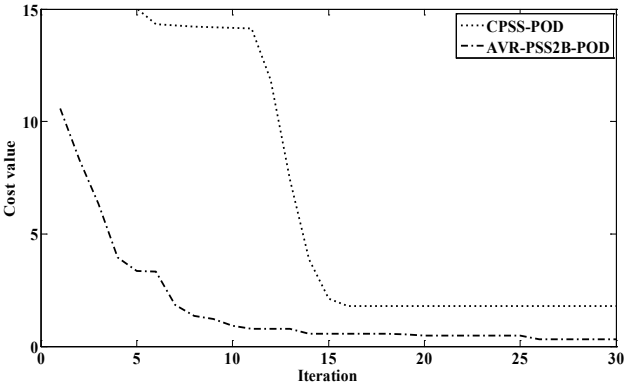


Fig. 8. Convergence profiles of the objective function for different controllers.

Table 6. EM modes of the 2A4M system without and with the coordinated controllers.

| | Coordinated controller | EM mode | Eigenvalue | Damping ratio |
|---|---|---|---|---|
| Operating condition 1 | No coordinated controller | Local1 | -0.6789±6.8807i | 0.0982 |
| | | Local2 | -0.7704±7.0459i | 0.1087 |
| | | Inter-area | 0.0232±3.0159i | -0.0077 |
| | CPSS-POD | Local1 | -2.1423 ± 8.3943i | 0.2473 |
| | | Local2 | -1.8261 ± 6.9427i | 0.2543 |
| | | Inter-area | -1.4412 ± 3.7312i | 0.3603 |
| | AVR-PSS2B-POD | Local1 | -2.2123 ± 5.1657i | 0.3937 |
| | | Local2 | -2.7106 ± 6.3635i | 0.3919 |
| | | Inter-area | -1.9328 ± 3.9672i | 0.4194 |
| Operating condition 3 | No coordinated controller | Local1 | -0.5869±6.9814i | 0.0838 |
| | | Local2 | -0.5609±7.3112i | 0.0765 |
| | | Inter-area | 0.0112±3.1457i | -0.0036 |
| | CPSS-POD | Local1 | -2.1423 ± 8.3943i | 0.2473 |
| | | Local2 | -2.0118 ± 8.2431i | 0.2371 |
| | | Inter-area | -1.4360 ± 3.671i | 0.3643 |
| | AVR-PSS2B-POD | Local1 | -2.7034 ± 6.4129i | 0.3885 |
| | | Local2 | -2.6192 ± 6.1523i | 0.3917 |
| | | Inter-area | -1.7112 ± 3.7538i | 0.4148 |

Table 4. Three operating conditions considered in our robust coordinated designs.

| | P1(MW) | Q1(Mvar) | P2 | Q2 | P3 | Q3 | P4 | Q4 |
|---|---|---|---|---|---|---|---|---|
| Operating condition 1 [3] | 700 | 185 | 700 | 235 | 719 | 176 | 700 | 202 |
| Operating condition 2 | 705 | 190 | 705 | 240 | 710 | 180 | 705 | 205 |
| Operating condition 3 | 710 | 195 | 710 | 245 | 730 | 185 | 710 | 210 |

Therefore, a perturbation in the system condition may result in heavy oscillations which can go on for a few seconds or even minutes before being damped or may bring about instability due to an unstable mode. In other words, it is necessary to employ a complementary damping controller to enhance the stability of this power system. Previously, the CPSS-POD coordination was applied [15] to alleviate the oscillation situation in this study. It can be observed from Table 6 that the proposed coordinated controller AVR-PSS2B-POD considerably outperforms the CPSS-POD coordination from the point of view of improved damping ratios and damping coefficients of the EM modes at different operating conditions. Consequently, overshoot, undershoot, and settling time indices can decrease in time domain simulations. Briefly, the eigenvalue analysis revealed that distinguished enhancement was achieved in the damping characteristics of the 2A4M system by applying the AVR-PSS2B-POD coordinated controller in comparison with the former CPSS-POD controller.

## 3.6 Time domain simulations

It has been stated in [3] that the linear controllers designed for power system oscillation stability enhancement should perform well enough under large disturbances. In this paper, the performance of the proposed comprehensive coordinated controllers was evaluated by both small and large disturbances. A step increase of 5% in the reference voltage $\Delta V_{ref}$ of the 1 and 4 generators at the instant of 10.0 sec was considered as a small disturbance. The time 10.0 s was selected to ensure that the starting transient conditions of the system were passed. For verifying the behaviour of the equipped power system under severe transient condition, a three-phase six-cycle (100 msec) fault (bolted three phase fault) at the middle of one of the parallel lines between bus 1 and 11 was cleared by disconnecting the line [15]. The robustness of the proposed controllers was evaluated by considering different operating points in the simulations. Accordingly, a comparative study on transient performance of the proposed controllers was conducted to choose the coordinated design with the higher damping performance. All time simulations were performed in a MATLAB/Simulink environment. The responses of rotor angles, inter-area and local mode oscillations, active power of machines, and power transfer from area 1 to area 2 were considered as outputs. These profiles are shown according to the base of the transmission line Sb=100 MVA, Vb=230 kV.

***Case I: Small-signal perturbation***

Figures 9(a) and 9(b) show the rotor angle responses of generators 1 and 4 under operating condition 1 for the small-signal perturbation where they were equipped with the proposed coordinated controllers. The applied increase in the reference voltages lead to a decrease in the rotor angles. In the base system, shown as "No coordinated controller" in the legend, the rotor angles oscillated highly over ten seconds with very poor damping. Although in the presence of the CPSS-POD controllers, the rotor angle profiles were improved, they still exhibited long settling time with high overshoot and undershoot that were unsatisfactory. By employing the proposed controller, significant damping enhancement occurred in the form of a decrease in settling time and overshoot and undershoot of the rotor angle signal in comparison with the profile of the CPSS-POD equipped system. As seen in Fig. 10(a) and Fig. 10(b), the local speed oscillation was damped very slowly and in the inter-area mode the amplitude of the oscillations increased, meaning that this mode was unstable.

The EM oscillations were mitigated to some extent by applying

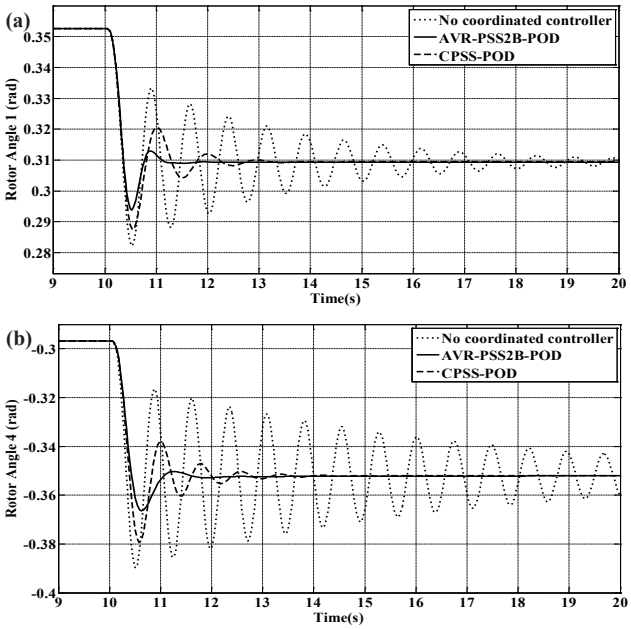


Fig. 9. Rotor angle of machines 1 and 4 for the small disturbance at the operating condition 1.

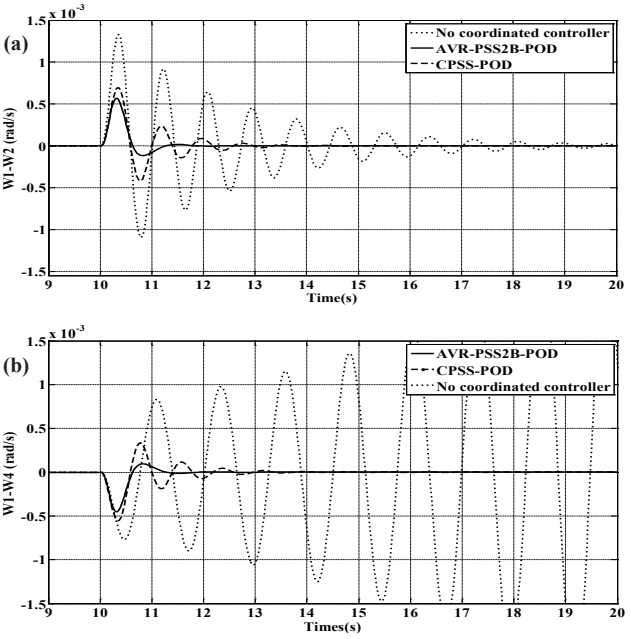


Fig. 10. Rotor speed responses for the small disturbance at the operating condition 1. (a) Local speed mode (ω1-ω2) and (b) inter-area mode (ω1-ω4).

the CPSS-POD controllers, although in the system equipped with our novel coordinated controller good results were obtained in damping of the EM oscillations.

As shown in Fig. 11(a) and Fig. 11(b), the CPSS-POD coordination could somewhat reduce the active power oscillations of machines 1 and 4. However, the settling time was still long with these controllers. It is clear that the system provided with the proposed controller, i.e., the AVR-PSS2B-POD, demonstrated remarkable responses in damping of the active power oscillations.

Figure 12 shows the profiles of active power transferred from

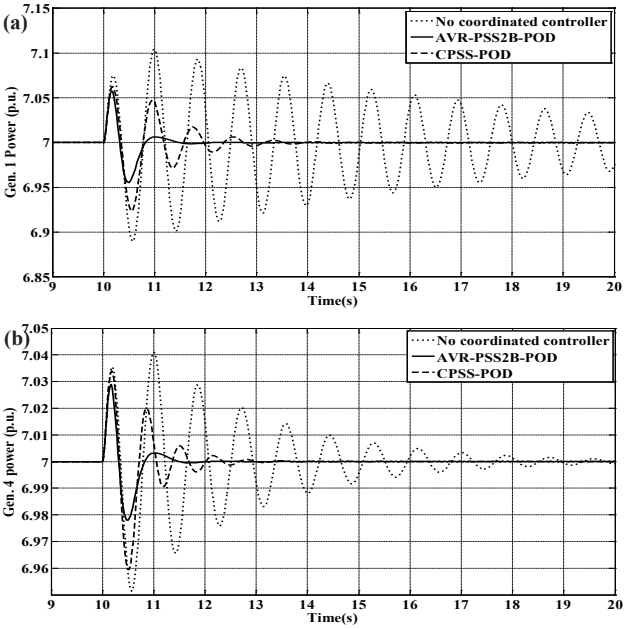


Fig. 11. Active power responses of machines 1 and 4 for the small disturbance at the operating condition 1.

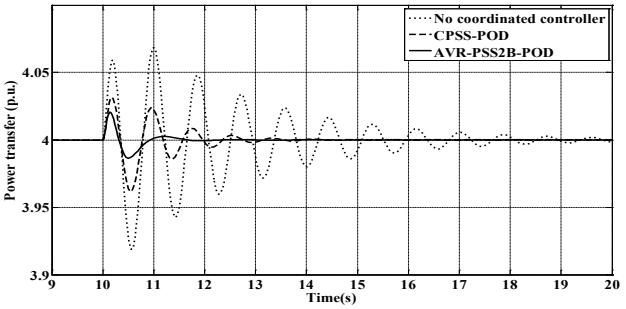


Fig. 12. Power transfer from area 1 to area 2 for the small disturbance at the operating condition 1.

area 1 to area 2 through the tie-line. It can be seen that the novelty of the proposed comprehensive coordination provides outstanding performance in damping of the power oscillations.

***Case II: Large-signal disturbance***

Figures 13(a) and 13(b) exhibit the rotor angle profiles of generators 1 and 4 for operating condition 3 under the applied large disturbance. As seen in Fig. 13, the transient fault leads to rotor angles oscillating highly with large overshoot and undershoot, which is undesirable from the point of view of oscillation stability. Thus, the system stability needs to be enhanced effectively. Although with the CPSS-POD controllers the oscillations have been diminished to some extent, damping indices of settling time, overshoot and undershoot are still high. By utilizing the proposed comprehensive coordination, significant damping improvement was achieved in comparison to the CPSS-POD controller. As seen in Fig. 14(a) and Fig. 14(b), severe EM oscillations were revealed due to the faulty condition. It can bring about system instability as a result of growing amplitude of the inter-area mode. These oscillations were reduced slightly by employing the CPSS-POD controllers. In order to obtain desirable damping characteristics, the proposed coordinated controller can contribute prominently in damping of the EM oscillations.

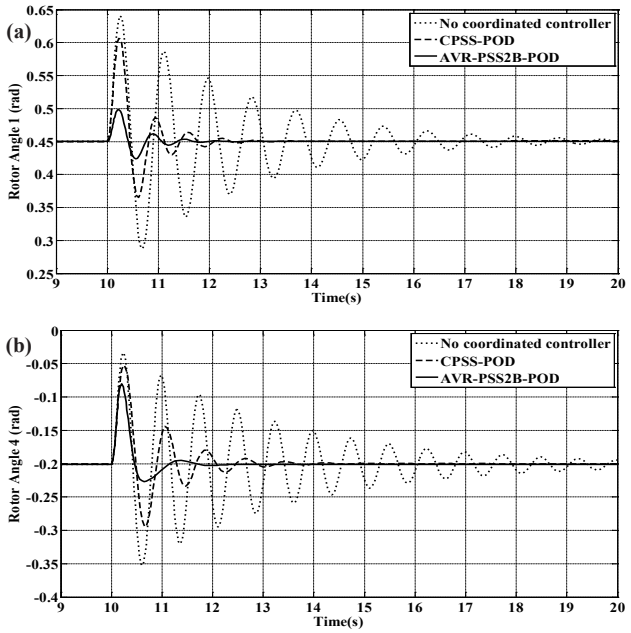


Fig. 13. Rotor angle of machines1and 4 for the large disturbance at the operating condition 3.

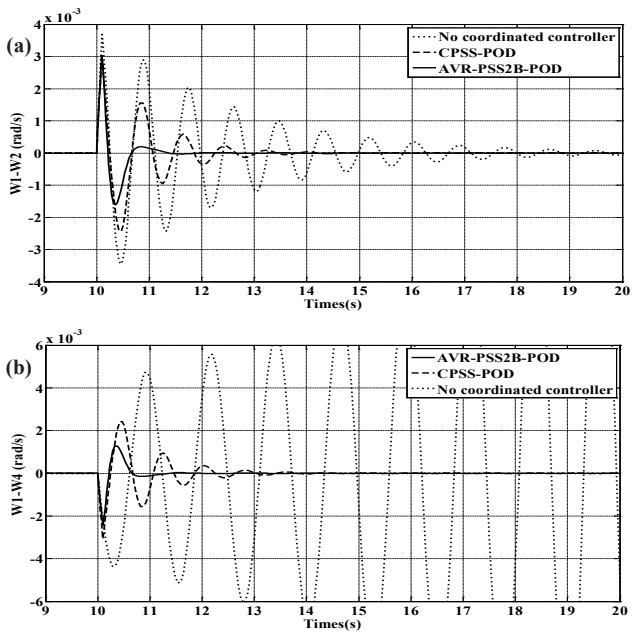


Fig. 14. Rotor speed responses for the large disturbance at the operating condition 3. (a) Local speed mode (ω1-ω2) and (b) inter-area mode (ω1-ω4).

It can be observed in Fig. 15(a) and Fig. 15(b) that the CPSS-POD coordination can decrease the active power oscillations of machines 1 and 4 to some degree; however, the oscillations settled slowly and also the amplitude of oscillations remained large. It is clear that the system equipped with the proposed controller showed good responses in damping of the active power swings. Figure 16 depicts the active power transferred between two areas. It is clear that effective damping performance can be acquired by equipping the system with the proposed coordinated controller. In the AVR-PSS2B-POD equipped system, the tie-line power oscillations have been suppressed remarkably.

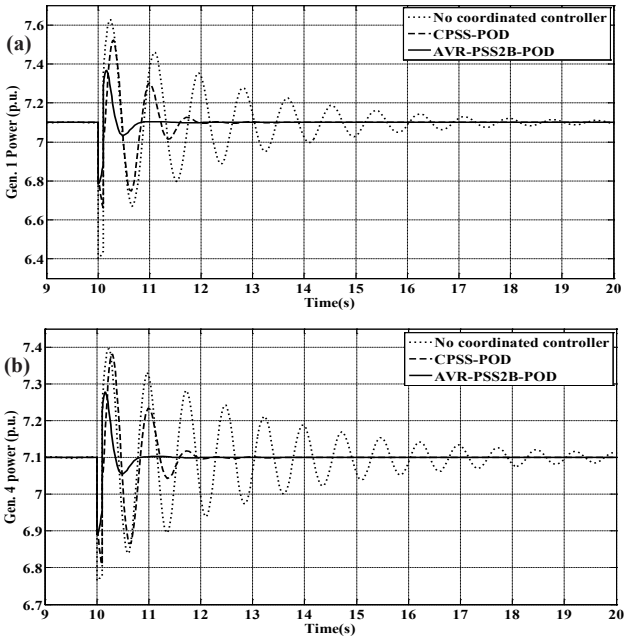


Fig. 15. Active power responses of machines 1 and 4 for the large disturbance at the operating condition 3.

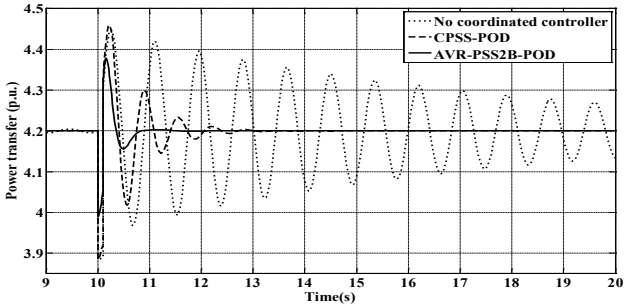


Fig. 16. Power transfer from area 1 to area 2 for the large disturbance at the operating condition 3.

## 4. LIST OF ABBREVIATIONS AND SYMBOLS

***A. ABBREVIATIONS***

| | |
|---|---|
| AVR | Automatic voltage regulator |
| CPSS | Conventional power system stabilizer |
| FACTS | Flexible ac transmission systems |
| TCSC | Thyristor controlled series capacitor |
| POD | Power oscillation damping |
| IPSO | Improved particle swarm optimization |
| GA | Genetic algorithm |
| EM | Electromechanical |
| PF | Participation factor |
| 2A4M | 2-area 4-machine |
| SMIB | Single machine infinite bus |

***B. SYMBOLS***

| | |
|---|---|
| $P_m$ | Mechanical input power of the generator |
| $P_e$ | Electrical output power of the generator |
| $P_{acc}$ | Accelerating power of the generator |
| $M(=2H)$ | Inertia constant of the generator |
| $D$ | Damping constant of the generator |
| $\delta$ | Rotor angle of the generator |
| $\omega$ | Rotor speed of the generator |
| $\omega_{eq}$ | equivalent speed of the generator |
| $\omega_b$ | Base speed |
| $E_{fd}$ | Field voltage |
| $T'_{do}$ | Field open circuit time constant |
| $E'_q$ | q-axis internal voltage behind the transient reactance of the generator |
| $x_d$ | d-axis reactance of the generator |
| $x'_d$ | d-axis transient reactance of the generator |
| $x_q$ | q-axis reactance of the generator |
| $K_A$, $T_A$ | Gain and time constant of the AVR |
| $K_S$, $T_S$ | Gain and inherent time constant of the TCSC |
| $V_{ref}$ | Reference voltage of the AVR |
| $V$ | Terminal voltage of the generator |
| $T_R$ | Measurement time constant of the terminal voltage |
| $T_{d1}$, $T_{d2}$, $T_6$, $T_7$ *(in PSS2B)* | Measurement time constants of channels of the stabilizers |
| $T_1$ *to* $T_{11}$ | Lead-lag time constants of the phase compensator blocks |
| $T_B$, $T_C$ | Time constants for possibility of representing transient gain reduction |
| $T_{B1}$, $T_{C1}$ | Time constants for possibility of representing transient gain increase |
| $K_F$, $T_F$ | Gain and time constant of the ST1A feedback path |
| $T_W$ | Washout time constants of the channels |
| $K_\omega$, $K_P$, $K_{S1}$, $K_{S2}$ | Gains of the stabilizers |
| $U_{PSS}$ | Stabilizing signal of the PSS |
| $U_{XTCSC}$ | Output signal of the POD controller |
| $U_{PSS}^{max}$, $U_{PSS}^{min}$ | Limiting values of the PSS output |
| $X_{TCSC}^{max}$, $X_{TCSC}^{min}$ | Limiting values of the TCSC output |
| $X_{TCSC}^{ref}$ | Reference reactance of the TCSC (which is commonly considered to be fixed) |
| $K_{pe}$, $T_m$ | Gain and measurement time constant of the POD controller |
| $[K_1]$ *to* $[K_6]$, $k_{px}$, $k_{qx}$, $k_{vx}$ | Coefficients of the modified Heffron-Phillips model |
| $A$ | State matrix of the system |
| $\Delta X$ | Total state vector of the system |
| $J$ | Objective function |

## 5. CONCLUSIONS

In this paper, in order to enhance multi-machine power system rotor angle stability, the coordination between CPSS and TCSC-based POD controller was developed to design three novel comprehensive coordinated controllers of AVR-PSS2B-POD. The comprehensive coordinated design means concurrent choice of the adjustable gains and time constants of the controllers. The eigenvalue analysis of the 2A4M power system revealed that the proposed IPSO-based comprehensive coordinated controller (AVR-PSS2B-POD) is much more capable than the CPSS-POD design to relocate the EM modes to improve the damping indices. Moreover, the results of time domain simulations performed for different operating conditions under small and large disturbances showed that the performance of the proposed coordinated controller is outstanding in damping of the power system oscillations, because damping indices such as overshoot, undershoot and settling time were effectively decreased in comparison with the CPSS-POD equipped system. Regarding the gain reduction capability of the static excitation system, incorporation of existing high-gain AVR in coordination with advanced dual-input PSS2B stabilizer and POD controller could outperform the earlier CPSS-POD controller in obtaining more desirable damping characteristics leading to a distinguished improvement in rotor angle stability of the power system.

## REFERENCES


[1] Y. N. Yu, *Electric Power System Dynamics* (New York, Academic Press, 1983).

[2] P. W. Sauer and M. A. Pai, *Power System Dynamics and Stability* (New Jersey: Prentice Hall, 1997).

[3] P. Kundur, *Power System Stability and Control* (New York: McGraw-Hill, 1994).

[4] G. Rogers, *Power System Oscillations* (Boston, Kluwer Academic, 2000).

[5] Y. Chompoobutrgool, L. Vanfretti, and M. Ghandhari, *Euro. Trans. Elect. Power*, **21**, 2098 (2011). [DOI: http://dx.doi.org/10.1002/etep.545]

[6] M. J. Gibbard, D. J. Vowles, and P. Pourbeik, *IEEE Trans. Power Sys.*, **15**, 748 (2000). [DOI: http://dx.doi.org/10.1109/59.867169]

[7] J. M. Kim and S. I. Moon, *Euro. Trans. Electr. Power*, **16**, 235 (2006). [DOI: http://dx.doi.org/10.1002/etep.82]

[8] A. D. Falehi, M. Rostami, and H. Mehrjardi, *Engineering*, **3**, 478 (2011). [DOI: http://dx.doi.org/10.4236/eng.2011.35055]

[9] A. Dysko, W. E. Leithead, and J. O'Reilly, *IEEE Trans. on Power Systems*, **25**, 413 (2010). [DOI: http://dx.doi.org/10.1109/TPWRS.2009.2036704]

[10] W. Du, H. Wang, P. Ju, and R. Dunn, *Euro. Trans. Elect. Power*, **20**, 833 (2010). [DOI: http://dx.doi.org/10.1002/etep.310]

[11] J. H. Chow, J.J.S. Gasca, H. Ren, and S. Wang, *IEEE Cont. Syst. Mag.*, **20**, 82 (2000). [DOI: http://dx.doi.org/10.1109/37.856181]

[12] IEEE Standard 421.5-2005 (ed. New York-USA: IEEE Power Engineering Society) (2006).

[13] A. Murdoch, S. Venkataraman, and R. A. Lawson, *IEEE Trans. Energy Conv.*, **14**, 1664 (1999). [DOI: http://dx.doi.org/10.1109/60.815121]

[14] B. K. Panigrahi, A. Abraham, and S. E. Das, *Computational Intelligence in Power Engineering*, **302** (Berlin Heidelberg: Springer-Verlag, 2010). [DOI: http://dx.doi.org/10.1007/978-3-642-14013-6]

[15] H. Shayeghi, A. Safari, and H. A. Shayanfar, *Energy Conv. Management*, **51**, 2930 (2010). [DOI: http://dx.doi.org/10.1016/j.enconman.2010.06.034]

[16] H. Shayeghi, H. A. Shayanfar, S. Jalilzadeh, and A. Safari, *Energy Conv. Management*, **50**, 2583 (2009). [DOI: http://dx.doi.org/10.1016/j.enconman.2009.06.009]

[17] A.T.A. Awami, Y.L.A. Magid, and M. A. Abido, *Int. J. Elect. Power & Energy Syst.*, **29**, 251 (2007). [DOI: http://dx.doi.org/10.1016/j.ijepes.2006.07.006]

[18] J. B. Park, Y. W. Jeong, J. R. Shin, and K. Y. Lee, *IEEE Trans. Power Electron.*, **25**, 156 (2010).

[19] F. P. D. Mello, L. N. Hannett, and J. M. Undrill, *IEEE Trans. Power Apparatus Syst.*, **PAS-97**, 1515 (1978). [DOI: http://dx.doi.org/10.1109/TPAS.1978.354644]

[20] A. Murdoch, S. Venkataraman, R. A. Lawson, and W. R. Pearson, *IEEE Trans. Energy Conv.*, **14**, 1658 (1999). [DOI: http://dx.doi.org/10.1109/60.815120]

[21] G. R. Berube, L. M. Hajagos, and R. Beaulieu, *Proc. IEEE PES Summer Meeting 1999* (Edmonton Alberta, Canada, 1999) p. 104-109 (1999).

[22] G. R. Berube, L. M. Hajagos, and R. Beaulieu, *IEEE Trans. Energy Conv.*, **10**, 532 (1995). [DOI: http://dx.doi.org/10.1109/60.464878]

[23] G.J.W. Dudgeon, W. E. Leithead, A. Dysko, J. O'Reilly, and J. R. McDonald, *IEEE Trans. Power Sys.*, **22**, 1986 (2007). [DOI: http://dx.doi.org/10.1109/TPWRS.2007.908404]

[24] R. You, *Ph. D. Thesis*, Montana State University, Montana (2006).

[25] M. M. Farsangi, Y. H. Song, and K. Y. Lee, *IEEE Trans. Power Sys.*, **19**, 1135 (2004). [DOI: http://dx.doi.org/10.1109/TPWRS.2003.820705]

[26] M. A. Abido, *Elect. Power Energy Syst.*, **22**, 543 (2000). [DOI: http://dx.doi.org/10.1016/S0142-0615(00)00027-2]

[27] R. M. Mathur and R. K. Varma, *Thyristor-based FACTS Controllers for Electrical Transmission Systems* (New York: IEEE Press and Wiley, 2002). [DOI: http://dx.doi.org/10.1109/9780470546680]

[28] M. P. Antonishen, H. Y. Han, T. K. Brekken, A. von Jouanne, A. Yokochi, D. A. Halamay, J. Song, D. B. Naviaux, J. D. Davidson, and A. Bistrika, *Proc. 2012 IEEE Power and Energy Society General Meeting* (San Diego, USA, 2012) p. 1-7.

[29] N. Bengiamin, L. Wang, and H. Salehfar, *Proc. 2000 IEEE Power Engineering Society Winter Meeting* (Singapore, 2000) p. 1331-1336.

[30] M. Sheikh, S. Muyeen, R. Takahashi, T. Murata, and J. Tamura, *Proc. IEEE Power Tech 2009* (Bucharest, Romania, 2009) p. 1-7.